Copper and zinc isotope compositions of pristine eucrites as analogues for differentiated planetary feedstocks

Jasmeet Dhaliwal, James M.D. Day, John Creech, Frédéric Moynier

Earth Planet. Sci. Lett. 637 (2024) 118740

Contents lists available at ScienceDirect

Earth and Planetary Science Letters

journal homepage: www.elsevier.com/locate/epsl

Copper and zinc isotope compositions of pristine eucrites as analogues for differentiated planetary feedstocks

Jasmeet K. Dhaliwal [a,b], James M.D. Day [a,*], John B. Creech [c], Frédéric Moynier [c]

[a] Scripps Institution of Oceanography, University of California San Diego, La Jolla, CA, 92093-0244, USA
[b] Earth & Planetary Sciences, University of California, Santa Cruz, CA, 95064, USA
[c] Université Paris Cité, Institut de Physique du Globe de Paris, Université, CNRS, 1 rue Jussieu, 75005, Paris, France

ARTICLE INFO

Keywords:
Eucrite meteorites
Copper
Zinc
Isotopes
Volatile depletion
Asteroid Vesta

ABSTRACT

Preferential enrichment of the heavier isotopes of moderately volatile elements (MVE) in samples from asteroids and the Moon have been attributed to volatile loss during the formation and differentiation of their parent bodies. Analogs for planetary feedstocks include the howardite-eucrite-diogenite meteorites, which originate from a differentiated planetesimal or planetesimals, likely including (4) Vesta. Complications arise in the interpretation of volatile depletion in these meteorites, however, due to post-crystallization processes including metamorphism and later impacts that acted upon them. We present new coupled Cu and Zn isotope data for a suite of eucrites that, when combined with published data, show significant ranges (δ^{65}Cu = -1.6 to +0.9‰; δ^{66}Zn = -7.8 to +13.5‰). Exclusion of eucrites that have been affected by metamorphism, impact contamination or surface condensation of isotopically light Zn and Cu leads to a range of 'pristine' compositions (δ^{66}Zn = +1.1 ± 2.3‰; δ^{65}Cu = +0.5 ± 0.5‰; 2 St. Dev.), implying inherent MVE variability within the eucrite parent body. As low-mass differentiated bodies, Vesta and the Moon represent endmembers in planet evolution. For the Moon, extensive volatile loss can be explained by a cataclysmic giant impact origin and later magma ocean crystallization. In contrast the parent body of eucrite meteorites likely heterogeneously lost volatile elements and compounds during differentiation. Vesta as the potential source of eucrite meteorites offers an important endmember composition for likely feedstocks to planets, representing the remaining vestige of what was likely to have been a larger population of differentiated objects in the inner Solar System shortly after nebula accretion. Mixing contributions of non-carbonaceous and carbonaceous chondrites constrained by nucleosynthetic Zn isotope anomalies suggests a significant fraction of Earth's accretion could have come from volatile-poor and differentiated planetary feedstocks that would have had limited effects on the bulk silicate Earth (BSE) Zn isotope composition. Furthermore, volatile-poor feedstocks cannot explain the BSE Cu isotope composition, which instead may have been modified by terrestrial core formation. Pristine eucrites offer key insights into early planetesimal differentiation and the role of volatile loss on small mass bodies within nascent solar systems.

1. Introduction

Volatile elements and compounds are critical for planetary evolution (e.g., Albaréde, 2009). Understanding the fate of volatiles within planetary bodies has been advanced through study of moderately volatile elements (MVE), which have 50% condensation temperatures (T_c) between 665 K and 1135 K at $<10^{-4}$ bar (Lodders, 2003). The MVE are proven tracers of volatile depletion events during planetary evolution and include elements such as zinc (Zn T_c = 726 K), copper (Cu T_c = 1037 K), potassium (K T_c = 1006 K) or sulfur (S T_c = 704 K) that experience limited isotopic fractionation during mantle melting (Chen et al., 2013; Labidi et al., 2013; Savage et al., 2015; Moynier et al., 2017; Day et al., 2022). Zinc, Cu, K and S have been extensively studied in lunar rocks (Moynier et al., 2006; Herzog et al., 2009; Paniello et al. 2012a; Wing and Farquhar, 2015; Wang and Jacobsen, 2016a; Tian et al., 2020; Day et al., 2017; 2019; 2020a; van Kooten et al., 2020; Gargano et al., 2022), as well as in achondrite meteorites, including howardite-eucrite-diogenite (HED) meteorites (Paniello et al. 2012b; Wu et al., 2018), with more limited analyses for angrites (Hu et al., 2022), aubrites (Moynier et al., 2011) and ureilites (Moynier et al., 2010; Brugier et al., 2019). Ubiquitous depletion in abundances and enrichment of the heavier stable isotopes of the MVE in these materials

* Corresponding author.
E-mail address: jmdday@ucsd.edu (J.M.D. Day).

https://doi.org/10.1016/j.epsl.2024.118740
Received 23 November 2023; Received in revised form 21 April 2024; Accepted 23 April 2024
Available online 6 May 2024

compared to chondritic values are indicative of isotopic fractionation during volatile loss, which occurs in a mass-dependent manner, in which lighter isotopes are preferentially subject to evaporation during kinetic processes. Determining when and how such volatile loss occurred is challenging because volatile loss processes are possible during nebular or planetary accretion, or due to magmatic differentiation or thermal events associated with impact, volcanism, or metamorphism on planets and planetesimals (e.g., Day and Moynier, 2014).

Within the Solar System, the Moon is significantly volatile depleted compared to Earth, evident in the low MVE abundances in lunar rocks compared to terrestrial rocks (e.g., Albaréde, 2009). During geological processes, element volatility can deviate from that expected from the T_c values, especially by variables such as oxidation state (Norris and Wood, 2017; Sossi et al., 2019). Furthermore, volatile loss experiments for Cu demonstrate significantly greater volatility of Cu at 2000 °C compared to Zn (Wimpenny et al., 2019; Day et al., 2020b; Sossi et al., 2020; Ni et al., 2021). This suggests that lunar isotopic measurements of these elements (Moon: δ^{66}Zn +1.4 ± 0.5; δ^{65}Cu = +0.92 ± 0.16‰; Day et al., 2019; 2020a) can be explained by the degree of vapor saturation, in which some portion of isotopically light Zn and Cu remains in the vapor. Depletion of the MVE in the Moon occurring at high degrees of vapor saturation would lead to suppressed kinetic fractionation during evaporative loss (Norris and Wood, 2017; van Kooten et al., 2020). In contrast, volatile loss on lower mass planetesimals was likely subject to more limited suppression, and therefore greater isotopic fractionation. As such, fully molten, low-mass and airless bodies are likely to lose volatile elements preferentially compared to larger bodies with significant atmospheres (Dhaliwal et al., 2018; Tang and Young, 2021; Charnoz et al., 2021). Given that those numerous asteroids and planetesimals are known to have melted and differentiated during the first few million years of the Solar System (Touboul et al., 2015), the feedstock planetesimals to the rocky inner planets could have included a significant fraction of volatile-poor differentiated objects. Hence, some fraction of accretion to bodies like Mercury, Venus, Earth, or Mars could have been depleted in volatile elements and the MVE in comparison with chondritic materials (Day, 2015). In turn, this form of accretion would have significant consequences for the likelihood of oceans, plate tectonics and habitability on planetary bodies.

Within the asteroid belt, there are several leftover planetesimal objects of significant size (> 100 km diameter). Some of these have not fully differentiated, such as Ceres (Russell et al., 2016), whereas others, like Vesta, have experienced differentiation into a core, mantle, and crust (McSween et al., 2019). The spectral association of HED meteorites with Vesta (Binzel and Zu, 1993) indicates that these meteorite samples are either directly or closely associated with differentiated planetesimal formation. Eucrite crystallization ages show that this differentiation occurred within the first ~1 to 5 million years of Solar System history (Touboul et al., 2015). An important aspect of eucrite meteorites is that they have variably experienced metamorphism and impact processes (Yamaguchi et al., 2011). Unbrecciated eucrites are some of the least modified crustal materials from Vesta (Mittlefehldt., 2015), and exhibit highly variable volatile element depletions compared to chondrites, with Antarctic eucrites being more depleted than non-Antarctic eucrites (Paniello et al. 2012b; Tian et al., 2019). To date, no MVE study has been able to properly consider the effect of post-crystallization processes on eucrites. These samples have experienced variable metamorphism or impact processes, which may be crucial for understanding the original volatile inventory of Vesta. Recent work has defined a 'pristinity' index for eucrites (Dhaliwal et al., 2023). We use this pristinity filter for eucrites to gain insights into how volatile depletions were generated in early-formed differentiated planetesimals, how Vesta compares with Earth, Mars and the Moon, and implications for volatile-poor planetary feedstocks.

2. Samples and methods

Sample powders investigated here have been previously measured for major- and trace-element abundances and associated polished thin-sections have been examined for petrography and petrology (Kumler and Day, 2021; Dhaliwal et al., 2023). Zinc and Cu isotope and abundance measurements were performed at the *Institut de Physique du Globe (IPGP), France* following protocols described previously (Savage et al., 2015; Moynier and Le Borgne, 2015). Isotopic compositions of Zn and Cu are reported as $\delta^{x}Zn = [(({}^{x}Zn/{}^{64}Zn)_{sample}/({}^{x}Zn/{}^{64}Zn)_{JMC\text{-}Lyon}) - 1] \times 1000$, for which $x = 66$, or 68, and $\delta^{65}Cu = [(({}^{65}Cu/{}^{63}Cu)_{sample}/({}^{65}Cu/{}^{63}Cu)_{NIST\text{-}SRM\text{-}976}) - 1] \times 1000$. Sample powders were dissolved in a 4:1 mixture of ultra-pure HF/HNO_3 in Teflon beakers for 96 h, dried down and then dissolved and further dried down in 6 M HCl twice to remove fluorides. Solutions were passed through columns to separate Zn and then Cu. Zinc purification was achieved using anion-exchange chromatography, with recovery of 99 ± 1%, and total procedural blanks <5 ng, representing <0.5% of total measured Zn (e.g., Moynier and Le Borgne, 2015). Samples and external standards were purified for Cu using a Bio-Rad AG MP-1 anion resin (Marechal et al., 1999; Savage et al., 2015), which, at low pH in chloride form, has a high partition coefficient for Cu. Sample aliquots were loaded onto the column and matrix elements were eluted in 8 ml of 7 N HCl. The Cu was then eluted in a further 22 ml of 7 N HCl. Samples were evaporated to dryness and the whole procedure was repeated to further purify Cu. The final Cu cuts were taken up in 0.1 N HNO_3 for analysis. The total procedural blank contained ~4 ng Cu, which equates to <1% of the Cu sample analyte.

Zinc isotopic and abundance compositions were measured on the *ThermoScientific* Neptune Plus multi collector-inductively coupled plasma-mass-spectrometer (MC-ICP-MS) housed at the IPGP. The Faraday cups were positioned to collect the masses 62, 63, 64, 65, 66, 67 and 68. Possible ^{64}Ni isobaric interferences were controlled and corrected by measuring the intensity of the ^{62}Ni peak. A solution containing 500 ng Zn in 0.1 M HNO_3 was prepared for isotopic analysis. This was done for Zn (and Cu) by first measuring a precisely diluted aliquot from the column chemistry to determine the abundance in the sample using the MC-ICP-MS and comparing with a 500 ng solution of the JMC-Lyon standard using ^{66}Zn (^{63}Cu), with a conservative estimate of uncertainty of ±10%. Isotopic ratios of Zn in all samples were analysed using a spray chamber combined with a 100 µl/min PFA nebulizer. One block of 30 ratios, in which the integration time of 1 scan was 10 s, were measured for each sample. The background was corrected by subtracting the on-peak zero intensities from a blank solution. The instrumental mass bias was corrected by bracketing each of the samples with standards. For reference, previously reported data for BHVO-2 yielded δ^{66}Zn 0.30 ± 0.03‰ (2 standard deviations [SD]), in good agreement with recommended values (δ^{66}Zn 0.24 ± 0.04‰, 2 sigma error [SE]; Moynier et al., 2017).

Copper isotope analysis was performed on the *ThermoScientific* Neptune Plus MC-ICP-MS following similar procedures to Savage et al. (2015). Samples were introduced into the instrument using an ESI PFA microflow nebuliser (50 µl min^{-1} flow rate) running into a quartz Scott double-pass spray chamber. The instrument was operated at low resolution (m/Δm ~1760, where Δm is defined at 5% and 95% of peak height), with the ^{65}Cu and ^{63}Cu beams collected in the C (central) and L2 Faraday cups, respectively. Matrix elements were monitored using ^{62}Ni and ^{64}Zn beams in L3 and L1 in the same cup set-up. Under typical running conditions, a 250 ng Cu solution generated a ca. 0.25 nA ion beam (i.e., ca. 25 V when combined with 10^{11} Ω amplifiers). Instrument background signal (typically <2 mV total Cu) was measured at the beginning and throughout each analytical session and subtracted from subsequent sample measurements. Isotope ratios were measured in static mode, with each measurement consisting of 25 cycles of 8.4 second integrations, with a three second idle time. Ratios were calculated in the Thermo Neptune Data Evaluation software, which discarded any outliers at the 2 SE confidence level. To correct for instrumental mass

bias, isotope measurements were calculated using the standard sample bracketing protocol relative to the NIST SRM976 standard. Analysis of two separate digestions of USGS standard reference material BHVO-2 gave δ^{65}Cu of 0.07 ± 0.06‰ (2SD), in good agreement with the recommended literature value (δ^{65}Cu = 0.12 ± 0.02‰; 2SE; Moynier et al., 2017). A generally higher Zn content is observed when measured by quadrupole ICP-MS than by MC-ICP-MS (*Table S1*), but Cu abundances measured by both techniques are similar.

3. Results

To investigate both the causes and extent of volatile depletion on differentiated planetesimals, isotopic and elemental abundances for Zn and Cu are reported for well-characterized and dominantly unbrecciated eucrite fractions for which major and trace elements, including Ni abundances, have been published previously (Dhaliwal et al., 2023). New Zn and Cu isotope and abundance data measured at the IPGP are reported for 23 eucrites (Table 1; *Table S1*). We also provide the full published Zn and Cu isotope dataset for eucrites, along with age information in *Table S2*. For the new data, Zn abundances range from 0.3 to 3.8 μg/g and copper contents range from 0.2 to 2.8 μg/g, apart from a fragment of Stannern, which has the highest Cu content of the dataset (11.6 μg/g) (Fig. 1). Zinc isotope compositions are mass-dependent with δ^{66}Zn values that range from −0.7 to +5.7‰ and fall within the range of Zn isotope compositions previously reported for eucrites (−7.8 to +6.3‰; Paniello et al. 2012b); δ^{65}Cu values span a more restricted range from −1.6 to +0.9‰ (Fig. 2).

Given the low Zn concentrations in most eucrites, only one measurement was possible for each sample. For comparison, the errors and values for repeat measurements of lunar samples using the same analytical techniques yield an error of ~10% on concentrations and 0.1‰ for δ^{66}Zn (e.g., Kato et al., 2015). For <4 μg/g Zn, there is a broad negative trend between Zn isotopic ratios and contents, in which eucrites with the heaviest and most positive δ^{66}Zn values have the lowest Zn contents (Fig. 2). For samples with >4 μg/g Zn, these is no strong variation in δ^{66}Zn. While the δ^{66}Zn of most samples with >4 μg/g Zn cluster around ~0‰, some possess negative δ^{66}Zn values likely indicative of recondensation from a vapor enriched in the lighter isotopes of Zn, as observed in some lunar samples (Day et al., 2017). For the eucrite dataset, this is most notable in sample PCA 82502 (δ^{66}Zn = −7.75‰). Antarctic unbrecciated eucrites measured in this study have a heavier Zn composition (δ^{66}Zn ~2‰) compared to non-Antarctic finds and falls, as well as the Antarctic brecciated eucrite, GRO 95533 (δ^{66}Zn ~0.55 ‰), but exhibit no clear trend with petrological type (*Table S2*). Given the more limited available Cu data for eucrites, no significant difference exists between Antarctic unbrecciated and non-Antarctic eucrites, or amongst petrological types. There are no correlations between Cu isotope compositions and abundances.

4. Discussion

4.1. Post-crystallization processes affecting MVE distributions in eucrites

As previously noted, no systematic differences in Zn or Cu isotope and abundances are observed between Antarctic and non-Antarctic falls and finds. Instead, Zn isotope data for eucrites have been interpreted to reflect initial compositional variation in Vesta superimposed by variations generated during bombardment by chondritic impactors (Paniello

Table 1
Zinc and copper isotope and abundance data for eucrite meteorites.

Sample	Type		Ni (μg/g)	Ni/Co	Zn (μg/g)	Cu (μg/g)	δ^{66}Zn	δ^{67}Zn	δ^{68}Zn	δ^{65}Cu	±
ALHA 81001	Antarctic Find	Unbrecciated	1.66	0.24	2.2	0.91	0.36	0.83	0.82	0.94	0.09
BTN 00300	Antarctic Find	Unbrecciated	0.96	0.15	0.3	0.91	*3.32*		*7.12*	−0.28	0.09
CMS 04049*	Antarctic Find	Unbrecciated	0.60	0.12	1.2	0.54	5.73	10.43	12.09		
EET 90020*	Antarctic Find	Unbrecciated	0.73	0.16	0.4	0.82	*6.22*		*12.45*	−0.66	0.07
GRA 98098	Antarctic Find	Unbrecciated	1.52	0.33	0.5	0.94	*6.18*		*12.35*	−1.46	0.01
LEW 85305	Antarctic Find	Unbrecciated	1.28	0.21	1.9	0.23	2.08	3.14	4.17		
PCA 82502	Antarctic Find	Unbrecciated	8.59	1.47	4.0	1.15	*−7.75*		*−15.14*	−0.39	0.08
PCA 91245*	Antarctic Find	Unbrecciated	0.71	0.13	1.6	0.88	−0.45	−0.50	−0.78	0.73	0.03
QUE 97014	Antarctic Find	Unbrecciated	0.69	0.18	1.3	1.82	1.93	3.12	3.99	0.17	0.05
QUE 97053*	Antarctic Find	Unbrecciated	1.49	0.71	3.1	0.65	−0.26	−0.32	−0.53	0.57	0.09
GRO 95533*	Antarctic Find	Brecciated	0.72	0.21	1.6	0.66	0.42	0.73	0.90	0.36	0.03
GRO 06059	Antarctic Find	Brecciated	42.1	4.97	0.6	0.66					
NWA 1000	Hot Desert Find	Impact Melt	4.76	0.50	1.7	0.48	0.64	1.02	1.31	0.51	0.08
NWA 1666	Hot Desert Find	Polymict Breccia	8.08	1.45	2.2	*1.85*	−0.42	−0.55	−0.80		
NWA 1836	Hot Desert Find	Polymict	1.50	0.20	1.6	1.43	0.40	0.68	0.89	0.26	0.09
NWA 1918	Hot Desert Find	Polymict	1.07	0.30	1.9	0.89	3.25	4.90	6.45	0.48	0.02
NWA 1923*	Hot Desert Find	Cumulate Eucrite	1.84	0.52	1.9	0.57	1.30	3.24	2.72	0.60	0.05
NWA 2362	Hot Desert Find	Polymict	2.75	1.06	1.6	0.83	1.08	1.90	2.22	0.23	0.06
NWA 5232	Hot Desert Find	Polymict Breccia	28.5	3.27	3.2	0.51	0.57	0.98	1.19	0.04	0.04
NWA 5356	Hot Desert Find	Polymict	0.72	0.14	1.6	1.35	1.29	2.79	3.30	0.86	0.07
NWA 5601	Hot Desert Find	Polymict Breccia	35.3	2.81	1.5	0.75	1.02	1.53	2.04		
NWA 5617	Hot Desert Find		3.79	0.86	1.4	0.59	1.36	2.61	3.08	0.80	0.02
Agoult	Fall	Monomict	2.26	0.39	0.9	0.33	1.60	2.53	3.34		
Bereba	Fall	Monomict	2.84	1.09	1.0	*1.35*	2.91	5.68	5.91		
Bouvante	Fall	Polymict	0.65	0.26	3.8	*2.77*	−0.73	−1.05	−1.41		
Juvinas	Fall	Monomict	18.8	2.75	1.4	0.70	*0.06*		*0.17*	−1.61	0.01
Millbillillie	Fall	Monomict	1.64	0.27	2.2	*1.43*	−0.02	0.12	0.07		
SaU 562	Fall	Unbrecciated	5.51	1.32	0.7	*1.84*				−1.11	0.05
Pasamonte	Fall	Polymict	4.73	0.86	2.0	*1.08*	0.98	1.70	2.02		
Stannern	Fall	Monomict	2.12	0.45	1.8	*11.62*	1.24	2.06	2.49		

*Samples are identified as pristine according to Dhaliwal et al. (2023); Ni and Ni/Co data are from the same reference. Antarctic eucrites are divided into brecciated or unbrecciated samples. Falls or hot desert finds are divided, in part, on whether they are brecciated or are monomict (consisting of a single lithology), polymict (consisting of multiple lithologies), a cumulate eucrite (NWA 1923) or are impact melts (NWA 1000). Classifications for these meteorites are taken from Dhaliwal et al. (2023).

Italicised values for Zn isotopes are from Paniello et al. (2012b).

Uncertainties shown for Cu are from repeat measurements of sample solutions and are either equal to or better than external uncertainties estimated from terrestrial standard reference materials (±0.06‰ 2 S.D.). Uncertainties for Zn isotope values based on terrestrial standard reference materials are ±0.03‰ (2 S.D.).

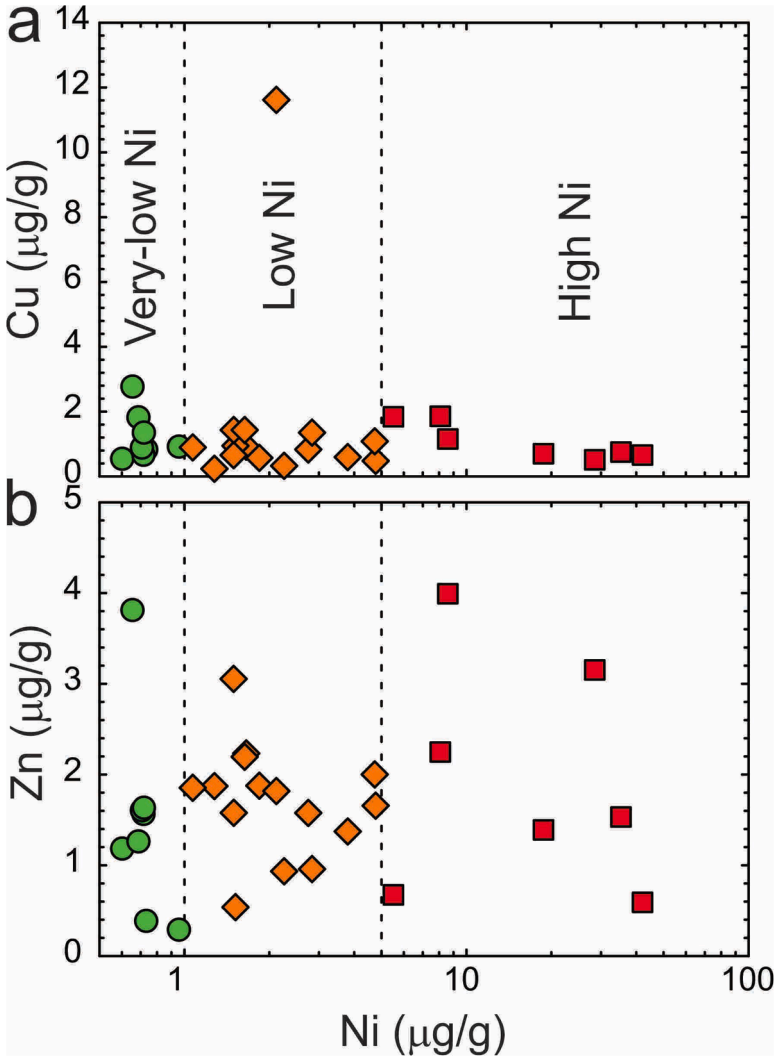

Fig. 1. **(a)** Copper and **(b)** Zn versus Ni abundances for eucrite meteorites (Table 1). Samples are divided into very-low bulk rock Ni (< 1 µg/g), low bulk rock Ni (1–5 µg/g) and high Ni (>5 µg/g), with the high Ni of some eucrites reflecting contamination by Ni-rich impactor material (after Dhaliwal et al., 2023).

et al. 2012b). For example, measured Zn and Cu abundances could conceivably reflect variable addition from iron meteorite-like impactors, which have lower concentrations of Zn and Cu compared with chondrites but would impart high Ni to samples. Clear evidence exists for impact modification to complex eucrite breccias, which can be composed of multiple basaltic lithologies (Mittlefehldt, 2015). Further, there is a rich record of impact on the surface of Vesta from remote sensing data of the DAWN mission (McSween et al., 2019). Indeed, impact-affected eucrites record younger ages compared with unbrecciated eucrites (*Table S2*). Given that absolute or relative age information is not comprehensive or standardized for eucrites, however, it is challenging to identify any trends for either Zn or Cu composition with existing chronological constraints.

Samples analysed here have been examined for post-crystallization effects (Dhaliwal et al., 2023). Eucrite samples considered pristine and free of post-crystallization effects are monomict (single lithology) and unbrecciated and have interstitial metal and sulfide grains that have low Ni/Co ratios and low siderophile abundances (<2 µg/g Ni, and "eucrite-like" W contents, typically 0.02 to <0.1 µg/g; Dhaliwal et al., 2023). These samples form a limited fraction of the suite of eucrites measured for Zn or Cu isotope composition; fragments of Bouvante, NWA 5356, QUE 97014, PCA 91245, CMS 04049, EET 90020 and BTN 00300 are considered pristine, within our dataset (Fig. 1). The compositions of these samples range in δ^{66}Zn from −0.73 to +6.2‰ and for δ^{65}Cu from –0.66‰ to +0.86‰ (Fig. 2). This is a significant range compared with mare basalts from the Moon that are unaffected by post-crystallization processes (δ^{66}Zn +1.4 ± 0.5; δ^{65}Cu = +0.92 ± 0.16‰; e.g., Day et al., 2019; 2020a). It is therefore possible to rule out impactor contamination, either from chondrites or iron meteorite impactors, as a major cause of Cu and Zn isotope or abundance variations in eucrites. We note that initial Zn and Cu contents within chondrite groups can be relatively large for a given Ni content (e.g., Phelan et al., 2022), but that Zn and Cu isotope variations of the extreme observed in eucrite meteorites are not possible (e.g., Moynier et al., 2011; Savage et al., 2022) (*Table S3*).

Zinc and Cu are potentially affected by a wide range of post-crystallization processes in eucrites, including vapor recondensation. For example, some lunar rocks have isotopically distinct Zn and Cu condensate on their surfaces (Day et al., 2017; 2019). It is also possible to recognize eucrite meteorites with condensate signatures, indicated by negative Zn and Cu isotope compositions (Fig. 2), likely resulting from local outgassing processes during emplacement of the magmas parental to eucrites to Vesta's surface environment. The volatile behavior of Zn and Cu enable these elements to become redistributed by melting, evaporation, and condensation processes.

A feature of the new data is that the lightest Zn and Cu isotope compositions typically do not occur in the same samples. This lack of correlation would suggest that post-crystallization processes do not lead

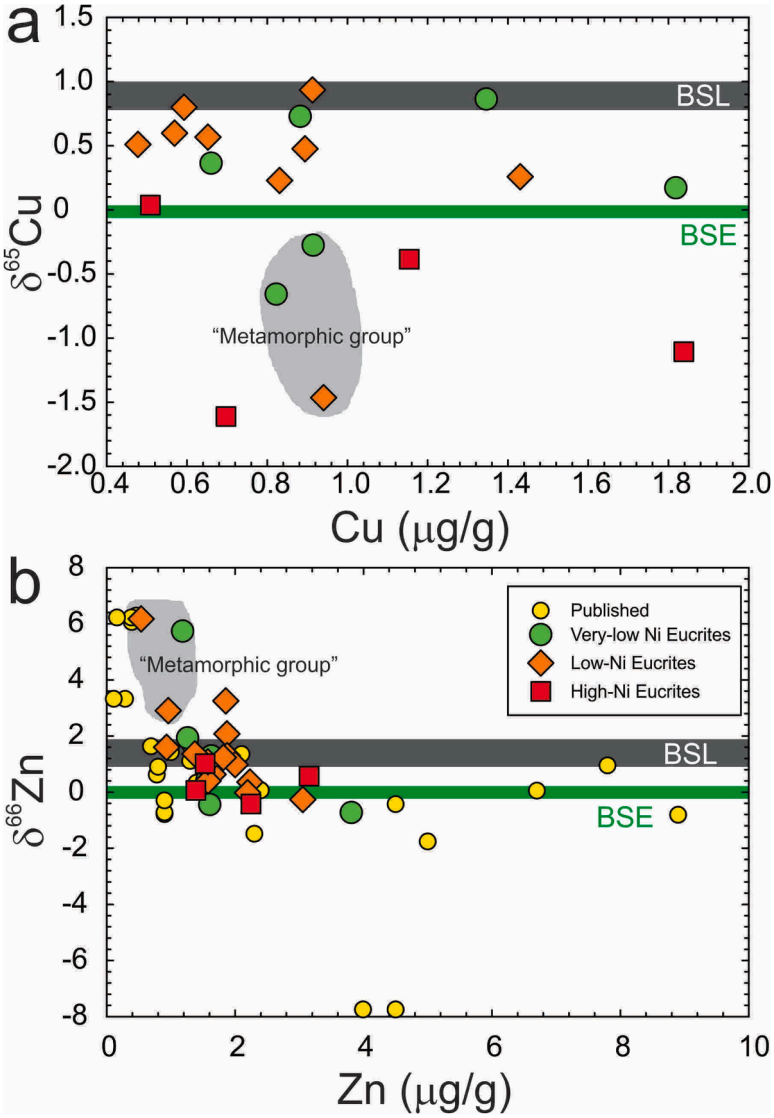

Fig. 2. **(a)** Copper and **(b)** Zn isotope and abundance compositions for eucrites from this study showing bulk rock Ni contents for the same sample powders and, for Zn, from Paniello et al. (2012a). Bulk silicate Earth (BSE) and Moon (BSL, L = lunar) estimates are from Paniello et al. (2012b) and Day et al. (2019). Error bars (2SD) are generally smaller than symbols (uncertainties on abundances are ~10% and on δ values are <0.1‰). Shown is the field for the metamorphic group (EET 90020, GRA 98098, BTN 00300) discussed in the text.

to coupled Cu-Zn isotope variability within eucrites, indicating differences in temperature conditions or the dominant mineralogy of condensed phases on the surface of individual eucrites (e.g., Renggli et al., 2017). Samples with low δ^{65}Cu can have high δ^{66}Zn, potentially indicating that after vaporization of both elements, intermediate temperatures between their condensation temperatures persisted. Zinc would continue to vaporize with preferential loss of light isotopes and lead to a heavier isotope composition, while the Cu vapor, enriched in light isotopes, would begin to condense, and lead to isotopically light signatures at the surface. These differences in volatility behavior are consistent with S concentrations (Wu et al., 2018) reported for different fragments of the same meteorites examine here, which covary negatively with Zn isotope composition but broadly positively with Cu isotopes (Fig. 3), consistent with predicted condensation behavior for these three elements.

4.2. Parent body processes and metamorphism

The new data demonstrates that consideration of post-crystallization processes that have acted on eucrites are required to properly interpret their MVE compositions. To examine the composition of bulk silicate Vesta (BSV), we assume that the most pristine, least post-crystallization affected eucrites are a proxy of its composition. The criterion for filtering for eucrites involves only those for which bulk rock Ni is reported on the same sample aliquot and where both Zn and Cu isotope data are available, and that are not impact melts (e.g., ALH 81001; NWA 1000; Kumler and Day, 2021). Taking samples with <5 μg/g Ni yields variability in δ^{66}Zn from −0.45 to 6.2‰ and δ^{65}Cu from −1.46 to +0.86‰; a more extreme filtration, to samples with <1 μg/g Ni yields the same variability in δ^{66}Zn (−0.45 to +6.2‰) and δ^{65}Cu from −0.66 to +0.86‰ (Fig. 4). Within the low Ni samples, EET 90020 has been shown to have been substantially affected by metamorphism (Yamaguchi et al., 2001) and, along with GRA 98098 and BTN 00300 are characterized by granular textures (Dhaliwal et al., 2023). These samples have the highest δ^{66}Zn and lowest δ^{65}Cu of the low Ni eucrite samples. The textures of these samples suggest that their Zn and Cu isotope signatures are a feature of Vesta's metamorphosed crust. The major reservoirs for Zn and Cu within eucrites are likely to be sulfide, spinel and high-Ca pyroxene phases (Kumler and Day, 2021). The metamorphosed sample group (EET 90020, GRA 98098; BTN 00300) show generally low Zn contents

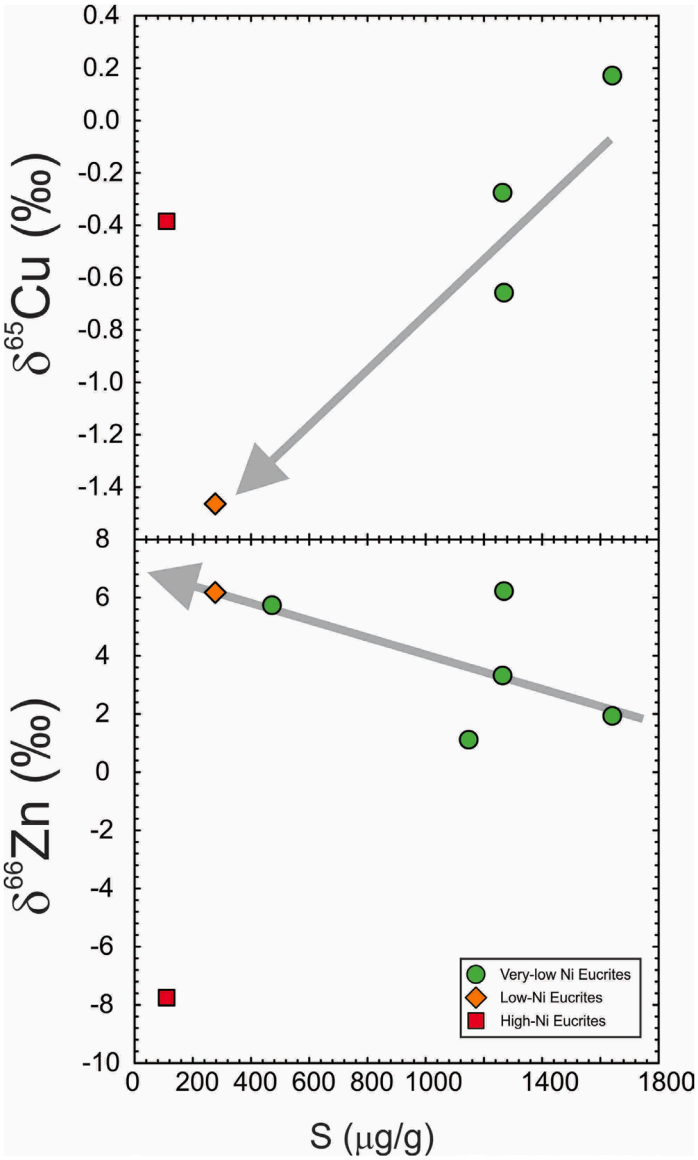

Fig. 3. Comparison of S content (Wu et al., 2018) versus Cu and Zn isotope data for eucrites and showing very-low, low and high-Ni designations from Fig. 1.

(<0.5 μg/g) and low Cu (<1 μg/g), but also have isotopically heavy S ($\delta^{34}S = +0.34$ to $+0.81$; Wu et al., 2018). It is notable that the S contents are variable and likely reflect 'nuggeting' of sulfide within measured samples. Metamorphism within Vesta's crust likely resulted in mobility of sulfide, and a trend towards light Cu and heavy Zn and S isotope compositions.

Filtering metamorphosed samples from the dataset results in a more restricted - but still large - range of compositions with ^{66}Zn from −0.45 to +3.25‰ and $\delta^{65}Cu$ from +0.17 to +0.86‰. The remaining 'pristine' and unmetamorphosed eucrites, which include Antarctic meteorites PCA 91245, QUE 97014 and QUE 97053, as well as hot desert finds NWA 1836, NWA 1918, NWA 1923, NWA 2362, NWA 5356 and NWA 5617 yield average [and weighted] bulk silicate Vesta $\delta^{66}Zn$ values of +1.1 ± 2.2‰ [+0.99‰] and $\delta^{65}Cu$ of +0.52 ± 0.51‰ [+0.48‰] (2SD). A conclusion arising from the consideration of post-crystallization processes acting on eucrites is that the wide ranges of Zn as well as Cu isotope data are probably inherent to the eucrite parent body(ies). Isotopic heterogeneity observed within individual fragments of some eucrite meteorites also suggests that the length-scale that post-crystallization processes, such as evaporation and condensation - engendered by metamorphism - could have operated on, were highly localized, even at the hand-specimen scale.

4.3. Comparisons with other MVE in eucrites

Isotope measurements of S and K are revisited in eucrites to evaluate their relations with Zn and Cu isotope compositions (*Table S2*); we also briefly consider H and Cl isotopes determined on mineral grains within eucrites (Sarafian et al., 2014; 2017; 2019; Wu et al., 2018; Tian et al., 2019; Barrett et al., 2016; 2019; Stephant et al., 2021). In this regard, it should be recognized that the K, Cu, Cl and H isotopes were not determined on the same sample aliquots used here or for establishing pristinity (Dhaliwal et al., 2023). Samples EET 90020, Bereba, Bouvante, Juvinas, Millbillillie, Pasamonte and Stannern all yield heavier K isotopic compositions (+0.44 ± 0.36‰; 2SD; Tian et al., 2019) than the bulk silicate Earth (BSE $\delta^{41}K \sim -0.48 \pm 0.03$‰; Wang and Jacobsen, 2016b) or lunar basalts ($\delta^{41}K$ of –0.07 ± 0.09‰; Tian et al., 2020). Notably, EET 90020, which has been metamorphosed, yields a heavier K isotopic composition, $\delta^{41}K = +0.68 \pm 0.06$‰, implying that K isotopes could also be affected by metamorphism, like Cu, Zn and S. Sulfur isotopes have been determined on BTN 00300, CMS 04049, EET 90020, GRA 98098 and QUE 97014, yielding $\delta^{34}S$ of +0.3 ± 0.6‰ (2SD),

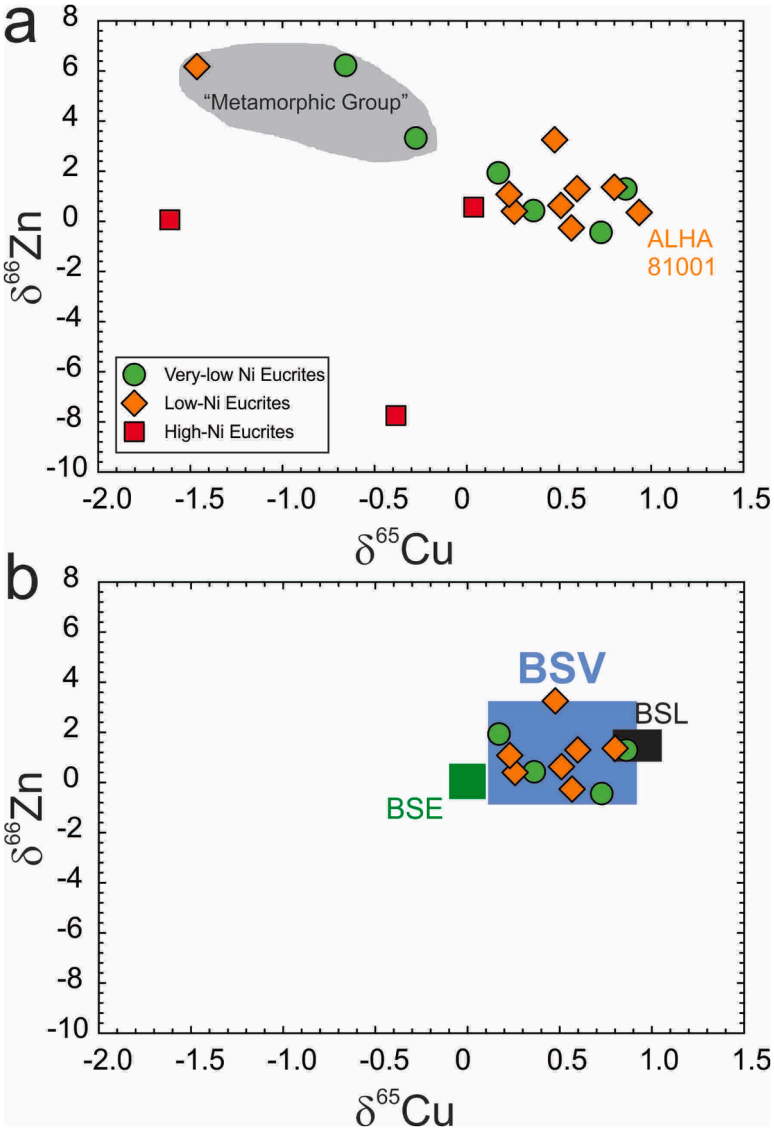

Fig. 4. Copper versus zinc isotope data for eucrite meteorites. In **(a)**, samples are shown with very low (<1 μg/g; green circles), low (1–5 μg/g; orange diamonds) and high (>5 μg/g; red squares) Ni contents. Outliers with very low to low Ni contents are ALHA 81001, which has an impact melt texture, and GRA 98098, EET 90020, and BTN 00300 that have granular textures characteristic of significant thermal metamorphism (Metamorphic Group), suggesting this process leads to lower δ^{65}Cu and higher δ^{66}Zn in samples, likely due to Zn loss and possible addition of isotopically light Cu from sulfide metasomatism. Shown in **(b)** are samples deemed as pristine and unaffected by disturbance of Cu or Zn. The BSE reservoir estimate is derived from terrestrial basalt data from Savage et al. (2015) and Moynier et al. (2017). Data for lunar basalts are from Paniello et al. (2012b), Moynier et al. (2006), Day et al. (2019).

trending to heavier values, but within uncertainty of chondrites (+0.07‰; Gao and Theimens, 1993). Excluding the metamorphosed eucrite group results in δ^{34}S of +0.1 ± 0.5‰ (2SD), within uncertainty of the chondrite value.

Chlorine and H isotope ratios have been measured in situ on apatite and pyroxene grains in eucrites. To date, only a limited number of samples have been analysed, with the majority showing indications of impact or thermal metamorphism modification. For example, apatite from Pasamonte, Millbillillie, Juvinas, Stannern, Agoult and GRA 98098 have been used to determine δ^{37}Cl values of −4 to +11.6‰ (Sarafian et al., 2017; Barrett et al., 2019). These samples, along with others measured for Cl and H isotopes in apatite grains (DaG 844, DaG 945, Moore County, NWA 1908, NWA 2362), from our calculations give mean weighted averages for δ^{37}Cl and δD of +1.7 ± 0.7‰ and -168 ± 134‰, respectively (Barrett et al., 2016; Sarafian et al., 2017), with the exception of apatite in GRA 98,098 that yields (δD = +126 ± 139‰). These values are likely to be higher than that predicted for potential accretion contributions to Vesta but are generally not as high as compositions for lunar rocks (McCubbin et al., 2023). Apatite or pyroxene will not be as susceptible to addition of surface condensate if they are within an igneous rock sample and will likely not be disrupted or modified by impacts unless significant thermal metamorphism or impact melting occurred (e.g., Kumler and Day, 2021). It is notable that pyroxene yields lighter δD values than apatite, with –263 ± 70‰ for Juvinas, Stannern, and Tirhert (Stephant et al., 2021), and –228 ± 49‰ for the Yamato meteorites (Sarafian et al., 2019). The more volatile-rich compositions of pyroxene may reflect their earlier crystallization within the basaltic crystallization sequence than apatite, which would record more significant late-stage magmatic degassing.

4.4. MVE depletion in the context of Vestan differentiation

The degree of variation of Cu and Zn isotopes within the eucrite parent body(ies) is large compared to estimates for BSE (δ^{66}Zn= +0.16 ± 0.06‰; Sossi et al., 2018; Day et al., 2022; δ^{65}Cu = +0.07 ± 0.10‰; Savage et al., 2015) or the bulk silicate Moon (BSL; δ^{66}Zn +1.4 ± 0.5‰;

$\delta^{65}Cu = +0.92 \pm 0.16‰$; Day et al., 2019; 2020a). Lunar mare basalts do not show the isotopic variation found in pristine eucrites. It is generally assumed that both Vesta and the Moon experienced large-scale magma ocean differentiation and degassing, with subsequent modification by impacts and metamorphism, both on global and local scales (e.g., Paniello et al. 2012a; Mittlefehldt, 2015). In the context of recent Cu volatility experiments (Sossi et al., 2020; Ni et al., 2021), differences in Cu isotopic compositions between eucrites and lunar samples are noteworthy. For example, if the Moon experienced a higher degree of vapor saturation compared to Vesta (Norris and Wood, 2017) it would also experience more limited isotopic fractionation for Zn and Cu. In the absence of vapor saturation, larger Zn and Cu isotope fractionations in HED meteorites would be expected. A caveat is that while the HED meteorites represent a diverse collection of falls and finds, most lunar rocks measured for Zn and Cu isotopic compositions are Apollo samples, and hence may be less spatially representative than eucrite samples but are not subject to issues of pristinity (low intrinsic highly siderophile elements e.g., Day et al., 2007).

Sulfur isotopic compositions in eucrites, which have been previously attributed to volatile loss (Wu et al., 2018), do not correlate with Zn or Cu isotope ratios, and may reflect differences in the origin and timing of volatile depletion for these elements. It is well-established that sulfur abundances in planetary mantles can be strongly affected by core formation (Steenstra et al., 2019), and that this process may also govern the partitioning of S isotopes (Labidi et al., 2013). While the Cu isotope composition of the BSL is not presently as well constrained as for Zn (Day et al., 2019), it has nonetheless been proposed that Cu may have been sequestered into the lunar core during sulfide segregation (Xia et al., 2019), leading to enrichment of the heavier isotope of Cu in BSL, which would not be expected for Zn (Mahan et al., 2017). Vesta is differentiated, possessing a relatively massive core (Russell et al., 2012) and being smaller than the Moon, likely underwent similar sulfide segregation processes at lower temperatures and pressures. The range of S isotope compositions in eucrites (Wu et al., 2018) is wider than in lunar samples (Wing and Farquhar, 2015), as it is for Cu isotopes. In the absence of post-crystallization metamorphic overprinting, if core formation in Vesta was responsible for sequestering isotopically light Cu, it did not impart a consistent Cu isotope signature to eucrites, which range from isotopically light to heavy values (Fig. 4).

4.5. *Implications for feedstocks to planets*

Comparison of estimates of $\delta^{41}K$, $\delta^{65}Cu$ and $\delta^{66}Zn$ for bulk silicate Earth (BSE), Moon (BSL) (Moon), Mars (BSM) and Vesta (BSV) are provided in Fig. 5. There is a relationship between surface gravity and K isotopes in inner Solar System objects (Tian et al., 2021), but this relationship is not clear for Cu and Zn isotopes. The uncertainties are larger for Zn in BSV than reported for K and would follow a generally similar trend of enrichment in the heavier isotopes with reducing surface gravity. In contrast, Cu shows no strong trend, with estimates for Cu isotopes for BSM currently lacking. Eucrites are isotopically heavier and have more variable ranges for Zn, and are broadly lighter for Cu, Cl and H (Sarafian et al., 2017) compared to BSL ($\delta^{41}K = \sim-0.07$, $\delta^{66}Zn = \sim+1.5‰$, $\delta^{63}Cu = \sim+0.9‰$) or in lunar mare basalts ($\delta^{37}Cl = \sim0$ to $+20‰$; $\delta D = \sim-300$ to $+1000‰$; Moynier et al., 2006; Sharp et al., 2010; Paniello et al. 2012a; Savage et al., 2015; Wing and Farquhar, 2015; Sarafian et al., 2017; Barnes et al., 2019; Day et al., 2020a). On the other hand, MVE abundance estimates for the BSV are broadly akin to BSL (Dreibus and Wanke, 1980; Davis, 2006).

The systematics noted above are significant given that magma ocean degassing models predict that smaller mass objects lose volatile elements preferentially (Dhaliwal et al., 2018), and hence should experience greater volatile depletion. The greater variability in MVE isotopic compositions of pristine eucrites compared to lunar mare basalts may support the notion that localized and more heterogenous volatile depletion processes occurred during Vesta's differentiation, potentially

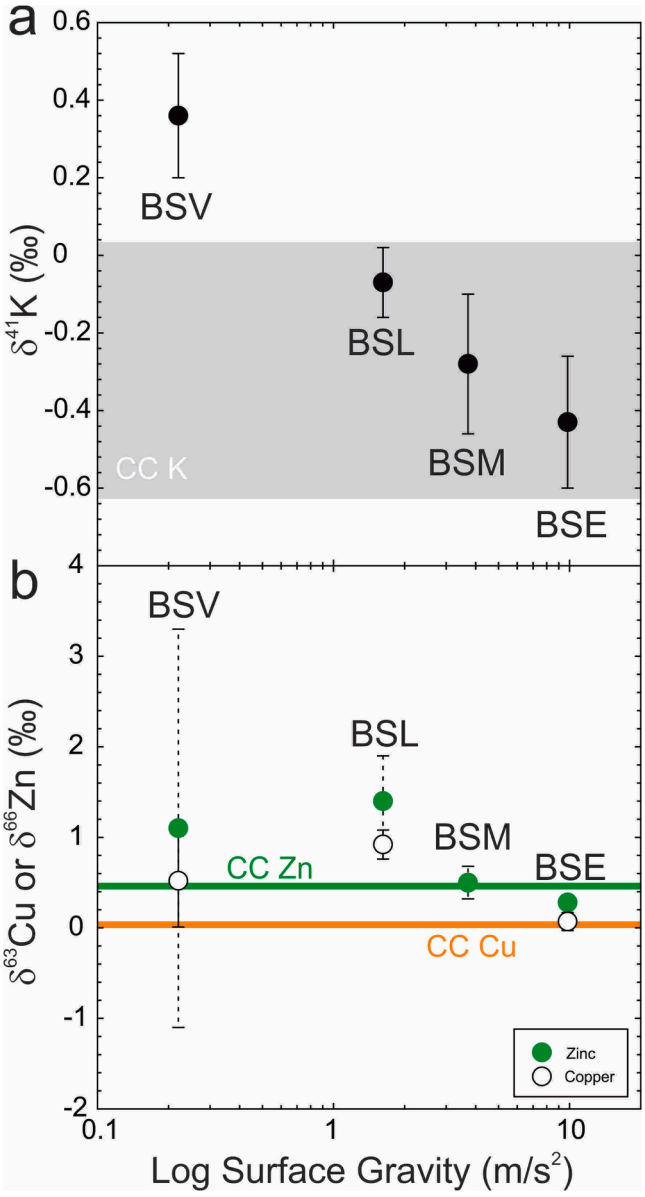

Fig. 5. Plots of surface gravity versus **(a)** average K, **(b)** Cu and Zn isotope data for Bulk Silicate Earth (BSE), Moon (BSL), Mars (BSM) and Vesta (BSV). Data for K isotopes are from Tian et al. (2021) with Cu and Zn data from this study (Vesta), Chen et al. (2013), Savage et al. (2015) (Earth), Day et al. (2019; 2020a) (Moon) and Paquet et al. (2023) (Mars). Average for carbonaceous chondrite (CC) Zn, Cu and K variations are shown in the respective figures. See *Table S3* for more information.

facilitated by a comparatively shallower magma ocean with more limited melting (Neumann et al., 2014; Mitchell et al., 2021; Dhaliwal et al., 2023), and was not limited by vapor saturation. On the other hand, the formation of the Moon in a giant impact may not be comparable to volatile depletion processes on smaller asteroid bodies given the Moon's gravity, with volatile loss from the Moon possibly being controlled by tidal effects with the Earth (Charnoz et al., 2021).

Models for planetary accretion show that feedstocks to inner Solar System planets, while broadly chondritic in composition, dominantly originated from the terrestrial planet forming region (Zhu et al., 2021), with the likelihood of both undifferentiated and differentiated bodies accreting to these bodies (Day, 2015; Carlson et al., 2018). An important constraint for planetary accretion models is whether differentiated bodies were anomalously volatile poor, having strong collateral effects

on the quantity of volatile elements and water delivery. Vesta is an important asteroid for examining volatile depletion in this regard, and our results suggest that, while some eucrites have MVE isotope compositions consistent with volatile depletion akin to lunar samples, overall isotopic fractionation of Cu and Zn for the Vestan crust was more heterogeneous than for the Moon.

It has previously been demonstrated that nucleosynthetic isotope anomalies offer a direct means for identifying the sources of material accreted by Earth. Nucleosynthetic isotope anomalies formed from presolar matter that was inhomogeneously mixed into the solar accretion disk (e.g., Steller et al., 2022; Savage et al., 2022). Mass balance calculations show that Earth has nucleosynthetic Zn isotope characteristics consistent with ~30% of the BSE Zn abundance deriving from a carbonaceous chondrite (CC) reservoir, with the remaining 70% originating from non-carbonaceous chondrite (NCC) components (e.g., Savage et al., 2022; Steller et al., 2022), although other studies have suggested a lower proportion of the CC reservoir (10%; Martins et al., 2023). Assuming a 30% CC contribution translates to ~6% of CC-like materials being added during Earth's accretion (Savage et al., 2022). From an MVE standpoint, if a three-component mixing assemblage is assumed considering volatile-rich (e.g., CC and NCC components) then 13% of an NCC component would be added leaving >80% of materials being potentially volatile-poor feedstocks.

In the following discussion, we assume that the composition of volatile-poor feedstocks directly matches that of BSV. The concentrations of Zn and Cu in pristine eucrites are typically <2 μg/g, respectively (Fig. 1). To determine a likely concentration in BSV, we assumed that Zn and Cu were incompatible in the melts and that even some pristine or metamorphosed eucrites may have higher Zn and Cu than after their eruption and crystallization. We therefore use 1 μg/g Zn and Cu for the BSV composition, but acknowledge that values could be as high as 2 μg/g. Mass balance calculations using 6% CC (CI chondrite), 13% NCC (enstatite chondrites) and 81% volatile-depleted components (BSV) reproduces the BSE Zn content of 55 μg/g Zn (*Table S3*) and would result in an average δ^{66}Zn for BSE of ~0.3‰, marginally higher than current estimates of BSE (+0.16±0.06‰; Sossi et al., 2018) and similar to prior estimates of BSE (+0.28±0.05‰; Chen et al., 2013) (Fig. 6). Performing this exercise assuming the same ratios of NCC (13%), CC (6%) and volatile-poor (81%) components for Cu would lead to an estimate BSE Cu content of 27.4 μg/g (versus the current estimate of 30 μg/g; *Table S3*) and δ^{65}Cu of around −0.14‰, substantially different from the BSE value of +0.07‰ (Savage et al., 2015).

An outcome of this exercise is that the limited abundances of Cu and Zn in volatile depleted feedstocks means that, despite their potential to dominate the absolute mass of accreted materials to planets, they have very limited leverage on the final isotopic compositional outcome of planets, meaning that such sources are also difficult to unambiguously detect using the MVE alone. Another noteworthy outcome of these

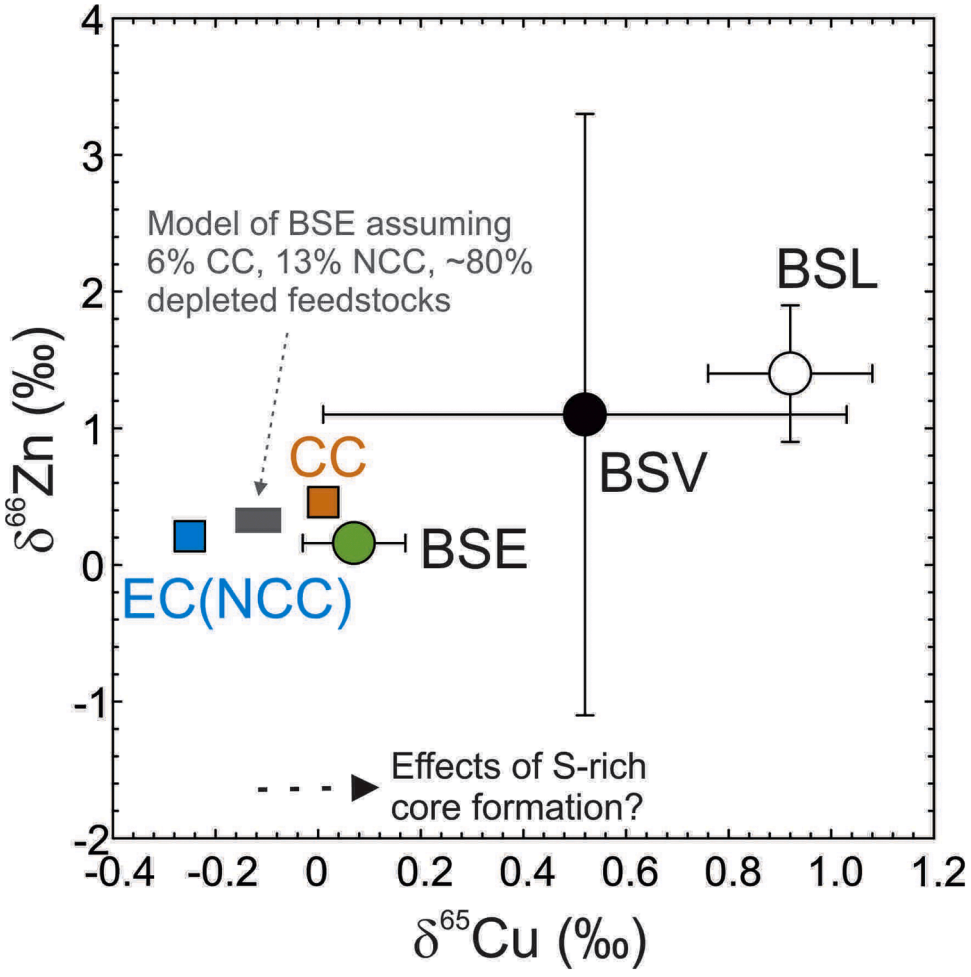

Fig. 6. Accretion estimates assuming mixing between 6% carbonaceous chondrite (CC) and 13% enstatite chondrite (EC, NCC) components with the remainder originating from depleted feedstocks, represented by pristine eucrites, or bulk silicate Vesta (BSV). The bulk silicate Earth (BSE) in such a model is strongly dominated by chondrite components for Cu and Zn, while the bulk silicate Moon (BSL) requires extreme depletion, consistent with volatile loss during lunar formation. These models indicate that initially depleted feedstocks to Earth-like planets could permissibly have accounted for a significant fraction of total accretionary materials. In detailed, modelled compositions do not match the BSE, especially for Cu isotopes, possibly reflecting fractionation during S-rich core segregation.

calculations is that the difference between the BSE δ^{65}Cu value and estimates from this study could relate to Cu sequestration into the core during sulfide segregation (e.g., Savage et al., 2015; Xia et al., 2019). A cautionary note, however, is that large uncertainties currently surround the Cu isotope values of feedstocks to the Earth and the variable volatile depletion that they are likely to have experienced. Notwithstanding the caveats, pristine eucrites provide an important end-member composition for understanding planetary accretion and the role of 'dry' differentiated planetesimals in the accretion of planets. Combined Cu and Zn isotope data for pristine eucrites suggests that differentiated planetesimals experienced significant and varied volatile loss and, as feedstocks to larger planets, would lead to MVE and – by inference – volatile poor accretion. Using such endmember compositions will be important in planetary accretion models, not just for the Solar System, but for exoplanetary systems.

5. Conclusions

Preferential enrichment in the heavier isotopes of MVE in samples from asteroids and the Moon have been attributed to volatile element loss during the formation and differentiation of their parent bodies. Analogs for planetary feedstocks include the HED meteorites, which originate from a differentiated planetesimal or planetesimals, likely including (4) Vesta. Complications arise in interpretation of volatile depletion in these meteorites, however, due to post-crystallization processes like metamorphism and later impacts that acted upon them. We present new coupled Cu and Zn isotope data for a suite of eucrites that, with published data, show significant ranges (δ^{65}Cu = −1.6 to +0.9‰; δ^{66}Zn = −7.8 to +6.3‰). Recognition and exclusion of eucrites that have been affected by metamorphism, impact contamination or surface condensation of isotopically light Cu, and so are considered pristine, leads to a range of compositions (δ^{66}Zn = +1.1 ± 2.3‰; δ^{65}Cu = +0.5 ± 0.5‰; 2 SD), implying inherent MVE variability with the eucrite parent body.

As low-mass differentiated bodies, Vesta and the Moon represent important endmembers in planet evolution. For the Moon, extensive volatile loss can be explained by a cataclysmic giant impact origin and later magma ocean crystallization. In contrast the parent body of eucrite meteorites likely heterogeneously lost volatiles during differentiation. Vesta as the potential source of eucrite meteorites offers an important endmember composition for likely feedstocks to planets, acting as the remaining vestige of what was likely to have been a larger population of such objects in the inner Solar System shortly after nebula accretion. Using pristine eucrites as the volatile-poor feedstock endmember and enstatite (NCC) and carbonaceous chondrites (CC) as undifferentiated accreted materials, suggests a significant contribution of volatile-depleted differentiated feedstocks could have accreted to form the Earth to account for the BSE composition.

CRediT authorship contribution statement

Jasmeet K. Dhaliwal: Writing – review & editing, Writing – original draft, Investigation, Formal analysis. **James M.D. Day:** Writing – original draft, Supervision, Project administration, Methodology, Investigation, Funding acquisition, Formal analysis, Data curation, Conceptualization. **John B. Creech:** Writing – review & editing, Validation, Methodology, Formal analysis. **Frédéric Moynier:** Writing – review & editing, Validation, Resources, Project administration, Methodology, Funding acquisition, Formal analysis, Data curation.

Declaration of competing interest

The authors declare no conflicts of interest.

Data availability

All data are included with the submission.

Acknowledgements

This work was supported by the NASA Emerging Worlds program (80NSSC19K0932) and an IPGP Visiting Professor position to JMDD. FM acknowledges the ERC grant 101001282 (METAL). Parts of this work were supported by IPGP multidisciplinary program PARI, by Region Île-de-France SESAME Grants no. 12015908, EX047016, and the IdEx Université de Paris grant, ANR-18-IDEX-0001 and the DIM ACAV+. Two anonymous reviewers are thanked for their constructive comments. We thank T. Kleine and J.A. Barrat, and K. Tait of the Royal Ontario Museum for the provision of falls and finds outside of Antarctica. For the Antarctic samples we thank the Meteorite Working Group. US Antarctic meteorite samples are recovered by the Antarctic Search for Meteorites (ANSMET) program which has been funded by NSF and NASA and characterized and curated by the Department of Mineral Sciences of the Smithsonian Institution and Astromaterials Curation Office at NASA Johnson Space Center.

Supplementary materials

Supplementary material associated with this article can be found, in the online version, at doi:10.1016/j.epsl.2024.118740.

References

Albarède, F., 2009. Volatile accretion history of the terrestrial planets and dynamic implications. Nature 461, 1227–1233.
Barnes, J.J., Franchi, I.A., McCubbin, F.M., Anand, M., 2019. Multiple reservoirs of volatiles in the Moon revealed by the isotopic composition of chlorine in lunar basalts. Geochim. Cosmochim. Acta 266, 144–162.
Barrett, T.J., et al., 2019. Investigating magmatic processes in the early Solar System using the Cl isotopic systematics of eucrites. Geochim. Cosmochim. Acta 266, 582–597.
Barrett, T.J., et al., 2016. The abundance and isotopic composition of water in eucrites. Meteorit. Planet Sci. 51, 1110–1124.
Binzel, R.P., Xu, S., 1993. Chips off of Asteroid 4 Vesta: evidence for the parent body of basaltic achondrite meteorites. Science 260, 186–191.
Brugier, Y.A., Barrat, J.A., Gueguen, B., Agranier, A., Yamaguchi, A., Bischoff, A., 2019. Zinc isotopic variations in ureilites. Geochim. Cosmochim. Acta 246, 450–460.
Carlson, R.W., Brasser, R., Yin, Q.Z., Fischer-Gödde, M., Qin, L., 2018. Feedstocks of the terrestrial planets. Space Sci. Rev. 214, 1–32.
Charnoz, S., Sossi, P.A., Lee, Y.N., Siebert, J., Hyodo, R., Allibert, L., Pignatale, F.C., Landeau, M., Oza, A.V., Moynier, F., 2021. Tidal pull of the Earth strips the proto-Moon of its volatiles. Icarus 364, 114451.
Chen, H., Savage, P.S., Teng, F.Z., Helz, R.T., Moynier, F., 2013. Zinc isotope fractionation during magmatic differentiation and the isotopic composition of the bulk Earth. Earth Planet. Sci. Lett. 369, 34–42.
Davis, A.M., 2006. Volatile Evolution and Loss. Meteorites Early Solar Syst. II 295–307.
Day, J.M.D., 2015. Planet formation processes revealed by meteorites. Geol. Today 31, 12–20.
Day, J.M.D., Moynier, F., 2014. Evaporative fractionation of volatile stable isotopes and their bearing on the origin of the Moon. Philos. Trans. R. Soc. A 372, 20130259.
Day, J.M.D., Pearson, D.G., Taylor, L.A., 2007. Highly siderophile element constraints on accretion and differentiation of the Earth-Moon system. Science 315, 217–219.
Day, J.M.D., Moynier, F., Shearer, C.K., 2017. Late-stage magmatic outgassing from a volatile-depleted Moon. In: Proceedings of the National Academy of Sciences, 114, pp. 9457–9551.
Day, J.M.D., Sossi, P.A., Shearer, C.K., Moynier, F., 2019. Volatile distributions in and on the Moon revealed by Cu and Fe isotopes in the 'Rusty Rock' 66095. Geochim. Cosmochim. Acta 266, 131–143.
Day, J.M.D., van Kooten, E.M.M.E., Hofmann, B.A., Moynier, F., 2020a. Mare basalt meteorites, magnesian-suite rocks and KREEP reveal loss of zinc during and after lunar formation. Earth Planet. Sci. Lett. 351, 115998.
Day, J.M.D., Moynier, F., Meshik, A., Pradivsteva, O., Wang, K., Petit, D., 2020b. Moderately volatile element behavior determined during nuclear detonation. Geochem. Perspect. Lett. 13. https://doi.org/10.7185/geochemlet.2014.
Day, J.M.D., Moynier, F., Ishizuka, O., 2022. A partial melting control on the Zn isotope composition of basalts. Geochem. Perspect. Lett. 23, 11–16.
Dhaliwal, J.K., Day, J.M.D., Moynier, F., 2018. Volatile element loss during planetary magma ocean phases. Icarus 300, 249–260.
Dhaliwal, J.K., Day, J.M.D., Tait, K.T., 2023. Pristinity and petrogenesis of eucrites. Meteoritics Planet. Sci. 58, 275–295.

Dreibus, G., Wänke, H., 1980. The bulk composition of the eucrite parent asteroid and its bearing on planetary evolution. Zeitschrift für Naturforschung A 35, 204–216.
Gao, X., Thiemens, M., 1993. Isotopic composition and concentration of sulfur in carbonaceous chondrites. Geochim. Cosmochim. Acta 57, 3159–3169.
Gargano, A., Dottin, J., Hopkins, S.S., Sharp, Z., Shearer, C., Halliday, A.N., Larner, F., Farquhar, J., Simon, J.I., 2022. The Zn, S, and Cl isotope compositions of mare basalts: implications for the effects of eruption style and pressure on volatile element stable isotope fractionation on the Moon. Am. Mineral. 107, 1985–1994.
Herzog, G.F., Moynier, F., Albarède, F., Berezhnoy, A.A., 2009. Isotopic and elemental abundances of copper and zinc in lunar samples, Zagami, Pele's hairs, and a terrestrial basalt. Geochim. Cosmochim. Acta 73, 5884–5904.
Hu, Y., Moynier, F., Bizzarro, M., 2022. Potassium isotope heterogeneity in the early Solar System controlled by extensive evaporation and partial recondensation. Nat. Commun. 13, 7669.
Kato, C., Moynier, F., Valdes, M.C., Dhaliwal, J.K., Day, J.M.D., 2015. Extensive volatile loss during formation and differentiation of the Moon. Nat. Commun. 6, 1–4.
Kumler, B., Day, J.M.D., 2021. Volatile element abundances in the asteroid Vesta determined from trace element distributions in eucrite meteorites. Geochim. Cosmochim. Acta 301, 211–229.
Labidi, J., Cartigny, P., Moreira, M., 2013. Non-chondritic sulphur isotope composition of the terrestrial mantle. Nature 501 (7466), 208–211.
Lodders, K., 2003. Solar system abundances and condensation temperatures of the elements. Astrophys. J. 591, 1220–1247.
Mahan, B., Siebert, J., Pringle, E.A., Moynier, F., 2017. Elemental partitioning and isotopic fractionation of Zn between metal and silicate and geochemical estimation of the S content of the Earth's core. Geochim. Cosmochim. Acta 196, 252–270.
Maréchal, C.N., Télouk, P., Albarède, F., 1999. Precise analysis of copper and zinc isotopic compositions by plasma-source mass spectrometry. Chem. Geol. 156, 251–273.
Martins, R., Kuthning, S., Coles, B.J., Kreissig, K., Rehkämper, M., 2023. Nucleosynthetic isotope anomalies of zinc in meteorites constrain the origin of Earth's volatiles. Science 379, 369–372.
McCubbin, F.M., Barnes, J.J., Ni, P., Hui, H., Klima, R.L., Burney, D., Day, J.M.D., Magna, T., Boyce, J.W., Tartese, R., 2023. Endogenous lunar volatiles. Reviews in Mineralogy and Geochemistry, 89, 729–786.
McSween Jr, H.Y., et al., 2019. Differentiation and magmatic history of Vesta: constraints from HED meteorites and Dawn spacecraft data. Geochemistry 79, 125526.
Mitchell, J.T., Tomkins, A.G., Newton, C., Johnson, T.E., 2021. A model for evolving crust on 4 Vesta through combined compositional and thermal modelling. Earth Planet. Sci. Lett. 571, 117105.
Mittlefehldt, D.W., 2015. Asteroid (4) Vesta: I. The howardite-eucrite-diogenite (HED) clan of meteorites. Geochemistry 75, 155–183.
Moynier, F., Le Borgne, M., 2015. High precision zinc isotopic measurements applied to mouse organs. JoVE (J. Visualiz. Exp.) 99, e52479.
Moynier, F., Albarède, F., Herzog, G.F., 2006. Isotopic composition of zinc, copper, and iron in lunar samples. Geochim. Cosmochim. Acta 70, 6103–6117.
Moynier, F., et al., 2010. Volatilization induced by impacts recorded in Zn isotope composition of ureilites. Chem. Geol. 276, 374–379.
Moynier, F., et al., 2011. Nature of volatile depletion and genetic relationships in enstatite chondrites and aubrites inferred from Zn isotopes. Geochim. Cosmochim. Acta 75, 297–307.
Moynier, F., Vance, D., Fujii, T., Savage, P., 2017. The isotope geochemistry of zinc and copper. Reviews in Mineralogy and Geochemistry 82, 543–600.
Neumann, W., Breuer, D., Spohn, T., 2014. Differentiation of Vesta: implications for a shallow magma ocean. Earth Planet. Sci. Lett. 395, 267–280.
Ni, P., Macris, C.A., Darling, E.A., Shahar, A., 2021. Evaporation-induced copper isotope fractionation: insights from laser levitation experiments. Geochim. Cosmochim. Acta 298, 131–148.
Norris, C.A., Wood, B.J., 2017. Earth's volatile contents established by melting and vaporization. Nature 549, 507–510.
Paniello, R.C., Day, J.M.D., Moynier, F., 2012a. Zinc isotopic evidence for the origin of the Moon. Nature 490, 376–379.
Paniello, R.C., et al., 2012b. Zinc isotopes in HEDs: clues to the formation of 4-Vesta, and the unique composition of Pecora Escarpment 82502. Geochim. Cosmochim. Acta 86, 76–87.
Paquet, M., Sossi, P.A., Moynier, F., 2023. Origin and abundances of volatiles on Mars from the zinc isotopic composition of Martian meteorites. Earth Planet. Sci. Lett. 611, 118126.
Phelan, N., Day, J.M.D., Dhaliwal, J.K., Liu, Y., Corder, C.A., Strom, C., Pringle, E., Assayag, N., Cartigny, P., Marti, K., Moynier, F., 2022. A ^{187}Re-^{187}Os, ^{87}Rb-^{87}Sr, highly siderophile and incompatible trace element study of some carbonaceous, ordinary and enstatite chondrite meteorites. Geochim. Cosmochim. Acta 318, 19–54.
Renggli, C.J., King, P.L., Henley, R.W., Norman, M.D., 2017. Volcanic gas composition, metal dispersion and deposition during explosive volcanic eruptions on the Moon. Geochim. Cosmochim. Acta 206, 296–311.
Russell, C.T., Raymond, C.A., Coradini, A., McSween, H.Y., Zuber, M.T., Nathues, A., De Sanctis, M.C., Jaumann, R., Konopliv, A.S., Preusker, F., Asmar, S.W., 2012. Dawn at Vesta: testing the protoplanetary paradigm. Science 336, 684–686.
Russell, C.T., Raymond, C.A., Ammannito, E., Buczkowski, D.L., De Sanctis, M.C., Hiesinger, H., Jaumann, R., Konopliv, A.S., McSween, H.Y., Nathues, A., Park, R.S., 2016. Dawn arrives at Ceres: exploration of a small, volatile-rich world. Science 353, 1008–1010.
Sarafian, A.R., Nielsen, S.G., Marschall, H.R., McCubbin, F.M., Monteleone, B.D., 2014. Early accretion of water in the inner solar system from a carbonaceous chondrite-like source. Science 346, 623–626.
Sarafian, A.R., John, T., Roszjar, J., Whitehouse, M.J., 2017. Chlorine and hydrogen degassing in Vesta's magma ocean. Earth Planet. Sci. Lett. 459, 311–319.
Sarafian, A.R., et al., 2019. The water and fluorine content of 4 Vesta. Geochim. Cosmochim. Acta 266, 568–581.
Savage, P.S., et al., 2015. Copper isotope evidence for large-scale sulphide fractionation during Earth's differentiation. Geochem. Perspect. Lett. 1, 53–64.
Savage, P.S., Moynier, F., Boyet, M., 2022. Zinc isotope anomalies in primitive meteorites identify the outer solar system as an important source of Earth's volatile inventory. Icarus 386, 115172.
Sharp, Z.D., Shearer, C.K., McKeegan, K.D., Barnes, J.D., Wang, Y.Q., 2010. The chlorine isotope composition of the Moon and implications for an anhydrous mantle. Science 329, 1050–1053.
Sossi, P.A., Nebel, O., O'Neill, H.S.C., Moynier, F., 2018. Zinc isotope composition of the Earth and its behaviour during planetary accretion. Chem. Geol. 477, 73–84.
Sossi, P.A., Klemme, S., O'Neill, H.S.C., Berndt, J., Moynier, F., 2019. Evaporation of moderately volatile elements from silicate melts: experiments and theory. Geochim. Cosmochim. Acta 260, 204–231.
Sossi, P.A., Moynier, F., Treilles, R., Mokhtari, M., Wang, X., Siebert, J., 2020. An experimentally-determined general formalism for evaporation and isotope fractionation of Cu and Zn from silicate melts between 1300 and 1500 C and 1bar. Geochim. Cosmochim. Acta 288, 316–340.
Steenstra, E.S., et al., 2019. Significant depletion of volatile elements in the mantle of asteroid Vesta due to core formation. Icarus 317, 669–681.
Steller, T., Burkhardt, C., Yang, C., Kleine, T., 2022. Nucleosynthetic zinc isotope anomalies reveal a dual origin of terrestrial volatiles. Icarus 386, 115171.
Stephant, A., et al., 2021. A deuterium-poor water reservoir in the asteroid 4 Vesta and the inner solar system. Geochim. Cosmochim. Acta 297, 203–219.
Tang, H., Young, E.D., 2021. Planetary evaporation. Elements 17, 401–406.
Tian, Z., Magna, T., Day, J.M.D., Mezger, K., Scherer, E.E., Lodders, L., Hin, R.C., Koefoed, R., Bloom, H., Wang, K., 2021. Potassium isotope evidence for a volatile-depleted early Mars. In: Proceedings of the National Academy of Science, 118, e2101155118.
Tian, Z., et al., 2019. Potassium isotopic compositions of howardite-eucrite-diogenite meteorites. Geochim. Cosmochim. Acta 266, 611–632.
Tian, Z., et al., 2020. Potassium isotopic composition of the Moon. Geochim. Cosmochim. Acta 280, 263–280.
Touboul, M., Sprung, P., Aciego, S.M., Bourdon, B., Kleine, T., 2015. Hf-W chronology of the eucrite parent body. Geochim. Cosmochim. Acta 156, 106–121.
Van Kooten, E., Moynier, F., Day, J.M.D., 2020. Evidence for transient atmospheres during eruptive outgassing on the Moon. Planetary Sci. J. 1, 67.
Wang, K., Jacobsen, S.B., 2016a. Potassium isotopic evidence for a high-energy giant impact origin of the Moon. Nature 538, 487–490.
Wang, K., Jacobsen, S.B., 2016b. An estimate of the Bulk Silicate Earth potassium isotopic composition based on MC-ICPMS measurements of basalts. Geochim. Cosmochim. Acta 178, 223–232.
Wing, B.A., Farquhar, J., 2015. Sulfur isotope homogeneity of lunar mare basalts. Geochim. Cosmochim. Acta 170, 266–280.
Wimpenny, J., et al., 2019. Experimental determination of Zn isotope fractionation during evaporative loss at extreme temperatures. Geochim. Cosmochim. Acta 259, 391–411.
Wu, N., Farquhar, J., Dottin III, J.W., Magalhães, N, 2018. Sulfur isotope signatures of eucrites and diogenites. Geochim. Cosmochim. Acta 233, 1–13.
Xia, Y., Kiseeva, E.S., Wade, J., Huang, F., 2019. The effect of core segregation on the Cu and Zn isotope composition of the silicate Moon. Geochemical perspectives letters 12, 12–17.
Yamaguchi, A., Barrat, J.-A., Ito, M., Bohn, M., 2011. Post-eucritic magmatism on Vesta: evidence from the petrology and thermal history of diogenites. Journal of Geophysical Research: Planets 116.
Yamaguchi, A., Taylor, G.J., Keil, K., Floss, C., Crozaz, G., Nyquist, L.E., Bogard, D.D., et al., 2001. Post-crystallization reheating and partial melting of eucrite EET 90020 by impact into the hot crust of asteroid 4Vesta ~4.50 Ga ago. Geochim. Cosmochim. Acta 65, 3577–3599.
Zhu, M.H., Morbidelli, A., Neumann, W., Yin, Q.Z., Day, J.M.D., Rubie, D.C., Archer, G. J., Artemieva, N., Becker, H., Wünnemann, K., 2021. Common feedstocks of late accretion for the terrestrial planets. Nature Astronomy 5, 1286–1296.